# Auger-Mediated Sticking of Positrons to Surfaces: Evidence for a Single-Step Transition from a Scattering State to a Surface Image Potential Bound State

S. Mukherjee,[1] M. P. Nadesalingam,[1] P. Guagliardo,[2] A. D. Sergeant,[2] B. Barbiellini,[3] J. F. Williams,[2] N. G. Fazleev,[1,4] and A. H. Weiss[1]

[1]*Department of Physics, University of Texas at Arlington, Arlington, Texas 76019, USA*
[2]*ARC Centre of Excellence for Antimatter-Matter Studies, School of Physics, The University of Western Australia, Crawley, WA 6009 Australia*
[3]*Department of Physics, Northeastern University, Boston, Massachusetts 02115, USA*
[4]*Department of Physics, Kazan State University, Kazan, 420008, Russian Federation*

(Received 21 December 2009; published 16 June 2010)

We present the observation of an efficient mechanism for positron sticking to surfaces termed here Auger-mediated sticking. In this process the energy associated with the positrons transition from an unbound scattering state to a bound image potential state is coupled to a valence electron which can then have sufficient energy to leave the surface. Compelling evidence for this mechanism is found in a narrow secondary electron peak observed at incident positron kinetic energies well below the electron work function.

DOI: 10.1103/PhysRevLett.104.247403 PACS numbers: 78.70.Bj, 03.65.Sq, 68.47.De, 71.60.+z

Recently, positrons [1] have been shown to be very effective in probing surfaces and reduced dimensional systems such as nanoparticles, which possess high surface-to-volume ratios. If positrons become trapped in image potential surface states before annihilation, they can provide a means of selectively sampling the top most layer of a material or nanostructure due to the fact that such states typically extend about one atomic layer below the surface. Subsequent annihilation of surface trapped positrons with core or valence electrons results in signals (e.g., annihilation induced Auger electrons [2] or annihilation gamma rays [3]) containing crucial information about the composition of the outermost regions of nanomaterials.

In this Letter, we present experimental evidence for an efficient quantum mechanism for depositing positrons directly into surface states through a single step. In this process, the energy associated with the positron transition from an unbound scattering state to a bound surface state is coupled to a valence electron which may then have sufficient energy to leave the surface. Because of its similarity with the Auger transition in solids, this process has been termed Auger-mediated sticking (AMS). The quantum nature of the AMS follows from the fact that the de Broglie wavelength of a 1 eV positron (about 12 Å) is an order of magnitude more than the width of the surface potential well (about 1 Å) [4]. Similar ideas have been suggested in theoretical models [5–7]; however, no experimental evidence of this mechanism was available until now. The AMS process schematized in Fig. 1 is related closely to the Auger deexcitation of atoms [8] or molecules [9] near surfaces, which has been studied for decades in various fields.

Here we provide direct experimental confirmation of the AMS process through measurements of electron energy spectra resulting from very low energy positron bombardment (1.5–7 eV). The strongest evidence for the AMS is found in a narrow electron peak observed at incident positron kinetic energies well below the electron work function value. The present experiment also allowed us to determine the positron sticking probability as a function of incident particle energy and to obtain an independent measurement of the positron binding energy at the surface [10]. The fact that this new mechanism has an efficiency exceeding 10% at positron energies ~1 eV proves that it will be possible to use low energy positron beams to selectively probe the surfaces of fragile systems such as nanoparticles and biomaterials and to obtain Auger signals which are completely free of secondary electron background.

The experiments were carried out using time of flight (TOF) positron annihilation induced Auger electron spec-

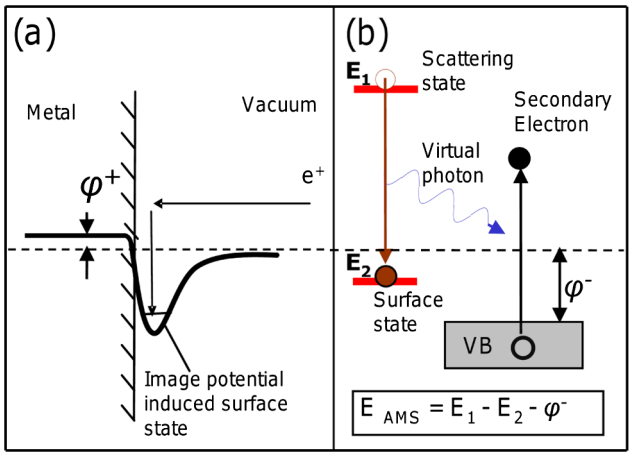


FIG. 1 (color online). Schematics of AMS process. (a) The slow positron in real space is directly trapped at the surface state resulting in the release of an electron carrying away the residual energy. (b) The energy band diagram showing the AMS [valence band (VB)].

 

trometer (PAES) [11], which uses a magnetic bottle analyzer [12]. Positrons from a Na-22 source are guided to the sample using **E** and **B** field. The emitted electrons are detected by a multichannel plate. The energy of the emitted electron was calculated from the electron TOF, which was determined from the time difference between the electron and annihilation gamma ray detections (see Ref. [11]). An Au sample (a 99.985% pure polycrystalline foil, 0.025 mm thickness) was sputter cleaned every 12 h while a Cu(100) sample (a 99.9% pure single crystal 10 mm diameter × 1 mm thickness) was sputter cleaned followed by annealing at 740 °C every 12 h. The incident beam profile at 0 V sample bias was fitted with a Gaussian of 0.4 eV FWHM and maximum at 0.65 eV. Ninety-nine percent of the positrons have energy less than 1 eV, which is referred to as the beam energy. The incident positron beam energy was increased by negatively biasing the sample.

The primary evidence for the AMS process in Cu is shown in Fig. 2(a), where the normalized energy spectrum taken at different positron beam energy $E$ (1.5–7 eV) is plotted. In each spectrum the large peak at low energies (<10 eV) corresponds to electrons that are emitted as a result of positron impact at the sample surface. The much smaller peak at about 60 eV is the PAES peak [2].

AMS can be distinguished from another process in which the final state of the incident positron is the bulk state. In the latter process, the maximum kinetic energy of the outgoing electron (as measured outside the sample surface) is given by

$$E_{\max} = E - \phi^- + \phi^+, \tag{1}$$

where $E$ is the incident positron energy (measured from the vacuum level) and $\phi^- = 4.65$ (4.8) eV is the electron work function in Cu (Au) and $\phi^+ = -0.02$ (+0.9) eV is the positron work function [13–16]. Both work functions are measured from the vacuum level with positive sign below the vacuum level. The electrons can escape the sample if $E_{\max} > 0$ eV, which implies that $E$ should be greater than $\phi^- - \phi^+$. Hence, for incident positron kinetic energies of less than 4.7 (3.9) eV there should be no secondary electron emission according to this mechanism. In the case of AMS, the positron excites an electron-hole pair while dropping to the surface state. The energy to dissipate is the initial positron kinetic energy plus the positron binding energy to the surface; thus, we have

$$E_{\max} = E + E_{ss} - \phi^-, \tag{2}$$

where $E_{ss}$ is the surface binding energy of the positron measured from the vacuum level (with positive sign below the vacuum). Annihilation induced processes including Auger transitions and $\gamma$-ray emission can lead to the emission of electrons with energies as high as the Auger transition energy and 511 keV, respectively. However, such processes would lead to the formation of broad electron peaks. In our experiments, we found a narrow electron peak even when the incident kinetic energies of the positrons were less than 3 eV. This can be explained from Eq. (2) by considering the process in which the electron excited from the Fermi sea escapes from the surface if the positron incident energy is greater than a certain threshold of about 2 eV since $E_{ss}$ is of the order of 3 eV in most metals [15].

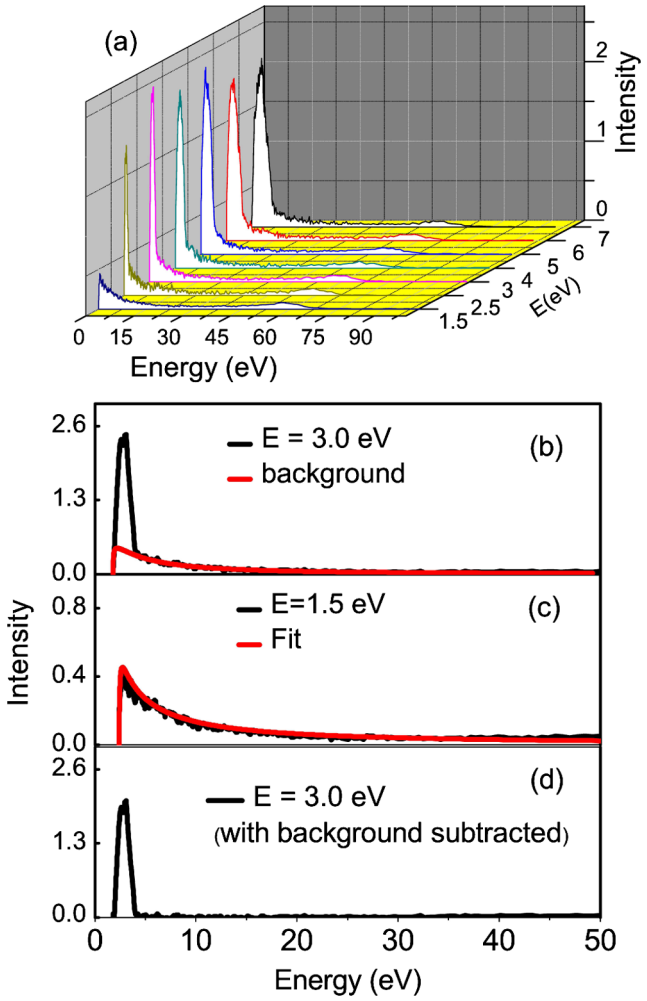


FIG. 2 (color online). Energy spectra of electrons emitted from Cu(100) resulting from low energy positron bombardment. (a) The spectra were taken for a series of positron energies ranging from 1.5 to 7 eV. All the data have been normalized to the Auger peak. (b) Electron energy spectrum taken with a beam energy of 3 eV. (c) Energy spectrum with a beam energy of 1.5 eV. (d) Same as (b) but with background, as estimated from (c), subtracted.

Figure 2(b) shows a typical electron spectrum of Cu. The large peak centered at 3 eV corresponds to AMS induced electrons. Figure 2(c) shows the spectrum similar to Fig. 2(b) except the beam energy is below the threshold for electron emission; thus, one can notice the absence of the low energy (AMS) peak: the sticking is still taking place, but electron emission outside the sample is energetically prohibited. The same broad background between 5–30 eV can be seen in both Figs. 2(b) and 2(c). This feature is presumably the low energy electron tail associ-

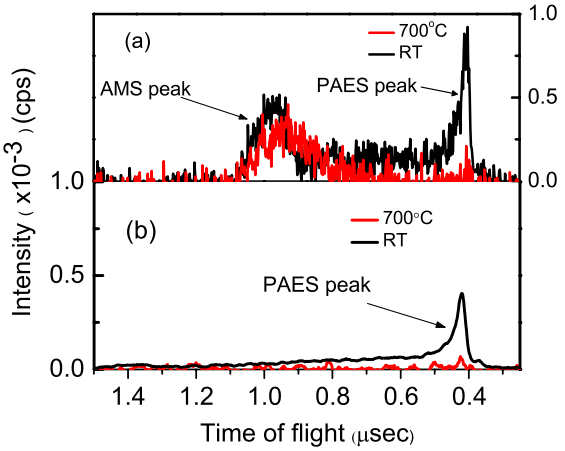


FIG. 3 (color online). Comparison of electron time of flight spectra, resulting from positron bombardment of hot and cold Cu(100) surfaces. (a) Cu at 700 °C and room temperature (RT) with a beam energy of 3 eV. (b) Same as (a) but with a beam energy of 1.5 eV. In (a) when the sample is at room temperature the incident positrons stick to the surface via AMS followed by annihilation with the core electrons resulting in PAES signal. When the positrons encounter the hot surface, they still undergo AMS but are desorbed as positronium before they can annihilate with core electrons [10] (note the inverted scale on TOF axis).

ated with the PAES peak at 60 eV. Figure 2(d) shows the same spectrum of Fig. 2(b) but with the PAES background subtracted.

As a test to determine whether the low energy peak (AMS peak) is due to a secondary effect of PAES or not, we have heated up the sample to 700 °C and performed measurements with incident positron beam energy above [Fig. 3(a)] and below [Fig. 3(b)] the threshold given by Eq. (2), respectively. At 700 °C, the positron trapped in the surface state is desorbed as positronium [15]. This prevents annihilation of the positron with core electrons and eliminates the PAES peak. Therefore, the presence of the AMS peak at high temperature in Fig. 3(a) proves that this feature is not associated with the PAES process. Finally, the PAES peak always disappears at high temperature [as shown in Figs. 3(a) and 3(b)] while the AMS peak disappears only when the beam energy is below threshold as given by Eq. (2).

The AMS peak integrated intensity with the background subtracted is plotted in Figs. 4(a) and 4(b) as a function of the incident positron energy and it is used to estimate the surface state binding energy $E_{ss}$. Previous measurements of $E_{ss}$ needed the monitoring of the fraction $f(T)$ of incident positrons which forms positronium as a function of sample temperature $T$ [10]. Here, we fit the low energy part (<5 eV) of the AMS peak integrated intensity with a linear function of the positron incident energy. The intercept of the straight line in conjunction with Eq. (2) is used to determine $E_{ss}$ for Cu ($2.79 \pm 0.2$ eV) and for Au ($2.87 \pm 0.22$ eV). This simple determination of $E_{ss}$ agrees well with values reported in the literature [16].

The AMS peak integrated intensity was also used to estimate the positron sticking probability $S(E)$. It has been assumed that the transition of the positron to the surface state is always associated with an electron-hole pair excitation. Hence, the sticking probability can be written as

$$S(E) = \frac{N_{\mathrm{AMS}}/N_{e+\mathrm{inc}}}{P(E)r(E)}, \tag{3}$$

where $N_{\mathrm{AMS}}$ is the integrated intensity of the AMS peak, $N_{e+\mathrm{inc}}$ is the number of incident positrons, $P(E)$ is the escape probability for the excited electrons [17], and $r(E)$ is that fraction of the excited electrons which have enough energy to escape by overcoming the work function $\phi^-$. The ratio $r(E)$ is therefore given by

$$r(E) = \frac{\int_{E_a}^{E_F} g(E)dE}{\int_{E_b}^{E_F} g(E)dE}, \tag{4}$$

where $E_F$ is the Fermi energy of the metal, $E_a = E_F - (E + E_{ss} - \phi^-)$, $E_b = E_F - (E + E_{ss})$, and $g(E)$ is the density of states [18]. The number of incident positrons $N_{e+\mathrm{inc}}$ was estimated using

$$N_{e+\mathrm{inc}} = N_{ss} + N_{Ps} + N_{\mathrm{ref}}, \tag{5}$$

where $N_{ss}$ is the number of positrons trapped in the surface state, $N_{Ps}$ is the number of positrons that form positronium, and $N_{\mathrm{ref}}$ is the number of positrons that are reflected from the surface. $N_{Ps}$ and $N_{ss}$ are related by $N_{Ps} = f(N_{ss} + N_{\mathrm{ref}})/(1 - f)$, where $f$ is the fraction of incident positrons that form positronium (~0.5, determined as in Ref. [10]), while $N_{\mathrm{PAES}} = CN_{ss}$ where $N_{\mathrm{PAES}}$ is the integrated intensity of PAES peak and $C$ is the probability that a positron trapped in the surface state will annihilate with a core electrons (4.6%) [14]. Taking 0.2 as the upper limit of $R = N_{\mathrm{ref}}/N_{e+\mathrm{inc}}$ [19], the total number of incident positron can be written as

$$N_{e+\mathrm{inc}} = \frac{N_{\mathrm{PAES}}}{0.8(1 - f - R)CT_{\mathrm{PAES}}}, \tag{6}$$

where $T_{\mathrm{PAES}} = 0.45$ (0.58) is the fraction of Auger electrons for Cu (Au) that are transmitted to and detected by our analyzer. The sticking probability $S(E)$ estimated in this way is plotted in Fig. 4(c), and its trend is consistent with the calculations by Walker *et al.* [7], especially for the Cu data. The reduced probability $S(E)$ observed for the Au data can be explained by a stronger screening. Walker *et al.* have used a screening parameter $\mu = 0.6\mu_{\mathrm{TF}}$ (where $\mu_{\mathrm{TF}}$ is the Thomas-Fermi screening parameter) in their calculation; however, in gold this parameter is bigger [20]. The prediction of Walker *et al.* that $S(E)$ will vanish as $E \rightarrow 0$ cannot be resolved by the present experiment. Here we are only interested in high positron surface sticking rates for nonzero positron energies.

We have reported experiments that provide strong evidence for a sticking process in which a low energy positron, incident on a surface, makes a direct transition from

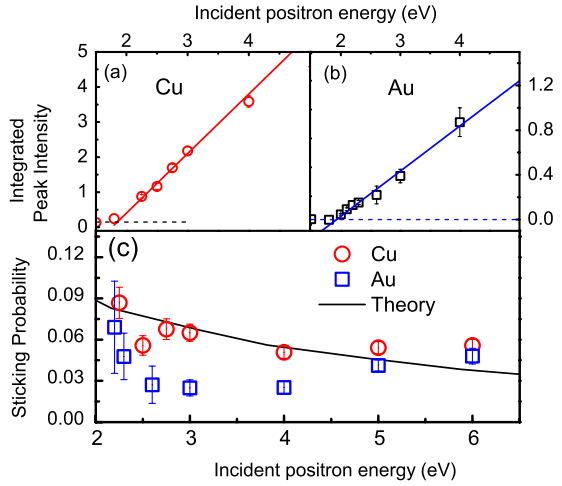


FIG. 4 (color online). AMS peak integrated intensity for (a) Cu and (b) Au as a function of incident positron energy. The data for positron energy less then 5 eV have been fitted with a straight line and the energy intercept has been used to determine the binding energy of the surface state [24]. The dashed line corresponds to the average background when the AMS process is energetically forbidden. (c) Sticking probability $S(E)$ calculated from Eq. (3). The theoretical calculation is from Ref. [7] and corresponds to a typical electron density of $r_s = 2$ a.u., $\phi^+ = -0.16$ eV, $E_{ss} = 3$ eV, and $\mu = 0.6\mu_{\mathrm{TF}}$.

an unbound scattering state into an image potential surface state, resulting in the emission of a secondary electron. We have termed this process Auger-mediated sticking (AMS) because the energy lost as the positron makes a transition to the bound state is given to an outgoing electron. Measurements of the incident beam energy at which the secondary peak first appears indicate a threshold almost 3 eV lower than the value that would be expected if the positron were making a transition to a bulk state. These measurements were used to obtain the first estimates of the surface state binding energy at room temperature. The AMS peak integrated intensity was used to estimate the sticking probability of positrons to surface and it is found to be in qualitative agreement with the theory [7]. Our measurements provide the first experimental demonstration of the trapping of positrons into the surface state with high efficiencies (~10%) at incident positron energies below the threshold for collision induced secondary electron generation (~1.5 eV). We have used this effect to obtain the first Auger spectra that are completely free of background due to primary beam induced secondary electrons. These measurements also demonstrate the possibility of greatly reducing the beam induced surface damage associated with Auger analysis by using incident positron energies below the threshold of chemical bond breaking [21]. The strong signal associated with the AMS process suggests that measurements of the AMS peak intensity as a function of energy can provide an independent way of testing models for inelastic scattering and sticking of light particles [22,23].

We acknowledge useful discussions with A. P. Mills, Jr., P. M. Platzman, and R. M. Nieminen. This work was supported in part by the NSF Grant No. DMR-0907679, Welch Foundation Grant No. Y-1100, the Ministry of Education and Science of the Russian Federation Grants No. 2.1.1/2985 and No. 2.1.1/3199, and the Australian Research Council Centre of Excellence Grant No. CE0561389. B. B. was supported by Contract No. DE-FG02-07ER46352 from the Division of Materials Science and Engineering, Office of Science, U.S. Department of Energy and benefited from the allocation of computer time at the NERSC and the Northeastern University's Advanced Scientific Computation Center.

[1] S. Eijt *et al.*, Nature Mater. **5**, 23 (2006).
[2] A. H. Weiss *et al.*, Phys. Rev. Lett. **61**, 2245 (1988).
[3] P. Asoka-Kumar *et al.*, Phys. Rev. Lett. **77**, 2097 (1996).
[4] A. P. Mills, Jr. *et al.*, Phys. Rev. Lett. **66**, 735 (1991).
[5] R. M. Nieminen, in *Positron Beam and Their Applications*, edited by P. G. Coleman (World Scientific, Singapore, 2000).
[6] M. J. Puska and R. M. Nieminen, Rev. Mod. Phys. **66**, 841 (1994).
[7] A. B. Walker *et al.*, Phys. Rev. B **46**, 1687 (1992).
[8] H. D. Hagstrum, Phys. Rev. **96**, 336 (1954).
[9] B. Barbiellini and P. M. Platzman, New J. Phys. **8**, 20 (2006).
[10] A. P. Mills, Jr., Solid State Commun. **31**, 623 (1979); K. G. Lynn, Phys. Rev. Lett. **43**, 391 (1979).
[11] S. Xie, Ph.D. thesis, UT Arlington, 2002.
[12] P. Kruit and F. H. Read, J. Phys. E **16**, 313 (1983).
[13] A. P. Knights and P. G. Coleman, Surf. Sci. **367**, 238 (1996); M. Farjam and H. B. Shore, Phys. Rev. B **36**, 5089 (1987).
[14] N. G. Fazleev *et al.*, Surf. Sci. **604**, 32 (2010).
[15] A. P. Mills, Jr., in *Physics with Many Positrons*, Proceedings of the International School of Physics "Enrico Fermi," Course LXXXIII, edited by W. Brandt and A. Dupasquier (Academic, New York, 1982).
[16] M. J. Puska and R. M. Nieminen, Phys. Scr. **T4**, 79 (1983).
[17] $P(E)$ is from Ref. [8] with $\alpha = 0.7$ and $\beta = 6$.
[18] We have assumed a constant density of states near $E_F$.
[19] J. A. Baker, M. Touat, and P. G. Coleman, J. Phys. C **21**, 4713 (1988).
[20] See, e.g., R. Saniz *et al.*, Phys. Rev. B **68**, 165326 (2003).
[21] A. H. Weiss *et al.*, Radiat. Phys. Chem. **76**, 285 (2007); A. H. Weiss, in Physics of Many Positrons, Proceedings of the International School of Physics "Enrico Fermi," Course CLXXIV (Institute of Physics, to be published).
[22] K. W. Goodman and V. E. Henrich, Phys. Rev. B **49**, 4827 (1994).
[23] A. P. Mills, Jr. and P. M. Platzman, in *New Direction in Antimatter Chemistry and Physics*, edited by Clifford M. Surko and Franco A. Gianturco (Dordrecht, Boston, 2001).
[24] The error bars are predominantly due to the uncertainty in the intercept as measured in Figs. 4(a) and 4(b).